Nrg1/ErbB Signaling-Mediated Regulation of Fibrosis After Myocardial Infarction

Manabu Shiraishi MD, PhD,[1,2] Atsushi Yamaguchi MD, PhD,[1] Ken Suzuki MD, PhD[2]

[1]Department of Cardiovascular Surgery, Saitama Medical Center, Jichi Medical University, Saitama 330-0834, Japan.

[2]William Harvey Research Institute, Barts and The London School of Medicine and Dentistry, Queen Mary University of London, London EC1M 6BQ, United Kingdom.

Short title: Regulatory mechanism of fibrosis after MI

Address correspondence to:

Manabu Shiraishi, Department of Cardiovascular Surgery, Saitama Medical Center, Jichi Medical University, Saitama 330-0834, Japan.

Tel: +81-48-647-2111; E-mail: manabu@omiya.jichi.ac.jp

Word count: 7864

Subject Terms

Cell signaling

Fibrosis

Ischemia

Myocardial Infarction

Abstract

RATIONALE: Appropriate fibrotic tissue formation after myocardial infarction (MI) is crucial to maintenance of the heart's structure. Reparative or M2-like macrophages play a vital role in post-MI fibrosis by activating cardiac fibroblasts. However, the mechanism by which post-MI cardiac fibrosis is regulated is not fully understood.

OBJECTIVE: We investigated the cellular and molecular mechanisms of post-MI fibrotic tissue formation, especially those related to regulation of cellular senescence and apoptosis.

METHODS AND RESULTS: *In vivo* and *in vitro* experiments were used to investigate the molecular and cellular mechanisms through which post-MI fibrosis occurs, with a focus on the role of M2-like macrophages. Microarray analysis revealed that $CD206^{+}F4/80^{+}CD11b^{+}$ M2-like macrophages collected from mouse hearts on post-MI day 7 showed increased expression of neuregulin 1 (Nrg1). Nrg1 receptor epidermal growth factor receptor ErbB was expressed on cardiac fibroblasts in the infarct area. In cardiac fibroblasts in which hydrogen peroxide-induced senescence, M2-like macrophage-derived Nrg1 suppressed both senescence and apoptosis of the fibroblasts, whereas blockade of ErbB function significantly accelerated. M2-like macrophage-derived Nrg1/ErbB/PI3K/Akt signaling, which was shown to be related to anti-senescence, was activated in damaged cardiac fibroblasts. Interestingly, systemic blockade of ErbB function in MI model mice enhanced senescence and apoptosis of cardiac fibroblasts and exacerbated inflammation. Further, increased accumulation of M2-like macrophages resulted in excessive progression of fibrosis in post-MI murine hearts. The molecular mechanism underlying regulation of fibrotic tissue formation in the infarcted myocardium was shown in part to be attenuation of apoptosis and senescence of cardiac fibroblasts by activation of Nrg1/ErbB/PI3K/Akt signaling.

CONCLUSIONS: M2-like macrophage-mediated regulation of Nrg1/ErbB signaling, ~~shown to~~ have a substantial effect on fibrotic tissue formation in the infarcted adult mouse heart, is critical for suppressing the progression of senescence and apoptosis of cardiac fibroblasts.

Key Words:

apoptosis; cardiac fibroblast; fibrosis; macrophage; myocardial infarction; senescence

Nonstandard Abbreviations and Acronyms

Akt protein kinase B

αSMA alpha-smooth muscle actin

BMDM bone marrow-derived macrophage

Cdk cyclin-dependent kinase

ErbB epidermal growth factor receptor

GEO Gene Expression Omnibus

Glb1 galactosidase beta 1

H_2O_2 hydrogen peroxide

IL-6 interleukin-6

MDM2 murine double minute 2

MI myocardial infarction

mTOR mechanistic target of rapamycin

M2 M2-like macrophage

Nrg1 neuregulin 1

Pdgfa platelet derived growth factor subunit A

71 **PI3K** phosphatidylinositol 3-kinase

72 **qRT-PCR** quantitative reverse transcription-polymerase chain reaction

73 **SA-β-gal** senescence-associated β-galactosidase

74 **SASP** senescence-associated secretory phenotype

75 **Spp1** secreted phosphoprotein 1

76 **Tgfb** transforming growth factor beta

77 **Thy1** thymocyte antigen 1

78

INTRODUCTION

Myocardial infarction (MI) is a leading cause of mortality and disability worldwide. Heart failure is common among survivors of acute MI, resulting from the adverse ventricular remodeling that follows MI.[1, 2] Because the regenerative capacity of the human heart does not fully compensate for the loss of cardiomyocytes that occurs with MI, formation of connective tissue is essential to maintenance of the integrity and rigidity of the heart. However, the mechanism by which cardiac fibrosis is regulated after MI is not fully understood.

MI results in permanent loss of hundreds of millions of cardiomyocytes.[3] Studies have shown that in the infarct area even non-cardiomyocytes, including fibroblasts, disappear in large quantities by apoptosis and that cellular senescence-associated defects occur in cardiac repair after MI.[4, 5] Apoptosis plays an important role in the disappearance of infiltrated immune cells and cardiac interstitial cells after MI.[5] Because senescence and apoptosis of both cardiomyocytes and fibroblasts are deeply involved in the pathophysiology of adverse left ventricular remodeling and myocardial rupture after MI,[6] understanding the molecular mechanisms by which senescence and apoptosis are regulated during the post-MI tissue repair process is important. Cellular senescence and apoptosis are processes of growth arrest that occur with age and in response to cellular stress and damage, and they limit proliferation of cells.[7, 8] Senescent cells possess a complex phenotype and are characterized by cell cycle arrest mediated via p16 and p53/p21 pathways, with some ultimately manifesting a unique secretory phenotype known as the senescence-associated secretory phenotype (SASP).[9] Cell cycle arrest plays a central role in the senescent phenotype of adult cardiomyocytes, and induction of cell cycle reentry of adult cardiomyocytes promotes post-MI cardiac repair.[10] Administration of anti-apoptotic substances to rats after MI has been shown to suppress cardiomyocyte apoptosis, which in turn decreases

102 infarct size and ameliorates the cardiac dysfunction that typically follows MI.[11] Even non-
103 cardiomyocytes in the infarct area, including fibroblasts, undergo apoptosis.[4, 5] Therefore,
104 senescence and/or apoptosis of cardiac fibroblasts may be involved in the tissue repair process
105 that follows MI. Senescent cardiac fibroblasts, in which expression of the major senescence
106 regulator p53 is significantly upregulated, have been shown to accumulate markedly in the
107 mouse heart after MI, with the upregulation of p53 shown to limit cardiac collagen production,
108 and conversely, the inhibition of p53 shown to increase reparative fibrosis.[1] However, the
109 methods used in the aforementioned studies are limited in their ability to identify the particular
110 subset of immune cells involved in the post-MI fibrotic process as well as the inherent cellular
111 and molecular mechanisms by which fibroblast senescence and collagen production are
112 regulated. Whereas fibrosis after MI is crucial to maintaining myocardial structure, excessive
113 fibrosis leads to eventual heart failure. Therefore, achieving equilibrium between profibrotic and
114 anti-fibrotic environments is important for a good regenerative outcome. For an understanding of
115 the fibrosis-based tissue repair process, intercellular communication between senescent and
116 apoptotic fibroblasts and surrounding immune cells must be clarified.
117 Investigators have shown macrophages to be essential for regeneration of the neonatal mouse
118 heart,[12] and we have shown that reparative or M2-like macrophages play a pivotal role in the
119 formation of fibrous tissue following MI by promoting proliferation and activation of cardiac
120 fibroblasts.[13] We hypothesized that M2-like macrophages play a vital role in attenuating
121 apoptosis and senescence of cardiac fibroblasts, both of which are profoundly involved in the
122 regulation of fibrotic processes after MI, and we investigated the molecular mechanism by which
123 this particular subset of immune cells effectuates this regulation.

124 Neuregulin 1 (*Nrg1*) is one of the neuregulin genes (*Nrg1–Nrg4*) belonging to the family of
125 epidermal growth factor genes,[14, 15] and Nrg1/epidermal growth factor receptor (ErbB) signaling
126 systems play essential roles in the protection and proliferation of cardiomyocytes in response to
127 injury.[16-19] Although association between Nrg1 and protection of cardiomyocytes has been
128 studied over several decades,[16-19] the exact mechanism through which Nrg1 protects cardiac
129 fibroblasts and the mechanism through which Nrg1 participates in post-MI regeneration have not
130 been elucidated. A recent study showed that Nrg1 enhances proliferation and viability of normal
131 human ventricular cardiac fibroblasts, with the Nrg1 activity linked to Nrg1/ErbB signaling.[20]
132 Results of a study in a mouse model of myocardial hypertrophy indicated that Nrg1 has an anti-
133 fibrotic effect in the heart, generated by anti-inflammatory Nrg1/ErbB signaling in
134 macrophages.[21] Furthermore, Nrg1-loaded poly-microparticles were used in a later study to
135 induce macrophage polarization toward an anti-inflammatory phenotype, which prevented their
136 transition toward the inflammatory phenotype and enhanced cardiac repair after MI.[22] However,
137 whether M2-like macrophages function to ameliorate senescence and apoptosis of cardiac
138 fibroblasts through Nrg1/ErbB signaling activity *in vivo* under post-MI conditions is unknown.
139 Although the contribution of Nrg1/ErbB signaling in macrophages and macrophage polarization
140 toward an anti-inflammatory phenotype to cardiac tissue repair was investigated in these studies,
141 the significance of Nrg1/ErbB signaling activity in cardiac fibroblasts with respect to the anti-
142 fibrotic effect of Nrg1 has not been clarified. We established what we believe to be an
143 appropriate *in vitro* model for delineation of the precise roles of M2-like macrophage-derived
144 Nrg1 after MI in anti-senescence, anti-apoptosis, and the fibrotic phenotype of fibroblasts.
145 Moreover, we used this model and an *in vivo* model to investigate the molecular and cellular
146 mechanisms by which post-MI fibrosis occurs, with a focus on the role of M2-like macrophages.

147 We aimed to shed light on the pathophysiology of fibrosis after MI and provide information that
148 will contribute to ultimate development of new therapeutic strategies that exploit Nrg1-driven
149 senescence and apoptosis of cardiac fibroblasts.
150
151 **METHODS**
152 **Data Availability**
153 The data that support the findings of this study are available from the corresponding author upon
154 reasonable request.
155 Microarray data: Gene Expression Omnibus GSE69879
156 (https://www.ncbi.nlm.nih.gov/geo/query/acc.cgi?acc=GSE69879)
157
158 Please see the Supplemental Materials for Methods and Major Resources.
159
160 **RESULTS**
161 **Cardiac Fibroblasts Undergo Apoptosis and Senescence After MI**
162 We investigated cellular senescence and apoptosis in a mouse MI model, which was established
163 by means of coronary artery ligation. Obvious fibrotic tissue formation and increased myocardial
164 expression of fibrosis-associated genes (*αSMA* [alpha-smooth muscle actin gene], *Col1a1*, and
165 *Col3a1*) were observed in the infarct area as soon as post-MI day 7 (Figure IA–B in the Data
166 Supplement). These changes were associated with an increase in the number of thymocyte
167 antigen 1 (Thy1)$^+$ fibroblasts and Thy1$^+$αSMA$^+$ myofibroblasts in the infarct area (Figure IC–D
168 in the Data Supplement), which peaked on post-MI day 7. Interestingly, approximately 40% of
169 Thy1$^+$ fibroblasts in the infarct area were positive for cleaved caspase 3 on post-MI day 7, and

170 approximately 15% were positive for cleaved caspase 3 on post-MI day 28, indicative of robust
171 apoptosis of cardiac fibroblasts (Figure 1A). Senescence-associated β-galactosidase (SA-β-gal)-
172 positive cells were also found in the infarct area. Numerous SA-β-gal-positive cells were spindle-
173 shaped and had many cytoplasmic processes and thus appeared to be fibroblasts (Figure 1B).
174 Additionally, myocardial expression of senescence-associated genes (*p16*, *p2*, and *Glb1* [beta 1
175 galactosidase gene])[1, 7, 8, 23, 24] and inflammation-associated genes (*CCL3*, *IL-6*, and *TNF*) was
176 upregulated in the infarct area in comparison to that in the non-infarct (remote) area (Figure 1C
177 and IE in the Data Supplement). Importantly, myocardial expression of reparative gene *Nrg1* was
178 upregulated in the infarct area, peaking on post-MI day 7 (Figure 1D). Immunohistochemistry
179 (IHC) showed that most Thy1$^+$ cardiac fibroblasts that had accumulated in both the infarct and
180 remote areas expressed ErbB2 and ErbB4, which are Nrg1 coreceptors[19, 25, 26] (Figure 1E). Taken
181 together, these results indicate that apoptosis and senescence of cardiac fibroblasts occur during
182 fibrotic tissue formation in the post-MI heart and that cardiac fibroblasts express 2 Nrg1
183 receptors, ErbB2 and ErbB4, in response to ischemic injury.
184
185 **M2-Like Macrophages Accumulate in the Infarct Area and Express Nrg1**
186 IHC showed that CD206$^+$ M2-like macrophages had accumulated in the infarct area, with peak
187 accumulation observed on post-MI day 7 (Figure 2A). Interestingly, this change in M2-like
188 macrophages corresponded to the change that occurred in cardiac fibroblasts after MI (Figure IC
189 in the Data Supplement). We further confirmed that CD206$^+$ cells were also positive for F4/80 in
190 both normal and infarcted hearts (Figure 2B). Microarray analysis showed that the molecular
191 signature of CD206$^+$F4/80$^+$CD11b$^+$ M2-like macrophages collected from infarcted hearts on
192 post-MI day 7 differed from that of M2-like macrophages collected from normal hearts (Figure

193 IIA in the Data Supplement). A range of anti-inflammatory and reparative genes was upregulated
194 in M2-like macrophages in comparison to expression of the same genes in M2-like macrophages
195 obtained from normal hearts (Figure IIB in the Data Supplement; the full dataset is available in
196 the Gene Expression Omnibus [GEO] database; GSE69879). Importantly, gene ontology analysis
197 showed association between M2-like macrophages obtained from infarcted hearts and regulation
198 of apoptosis and cell death (Figure IIC in the Data Supplement). By searching HomoloGene
199 (https://www.ncbi.nlm.nih.gov/homologene) for genes related to proliferation and viability, we
200 focused on the increased expression level of *Nrg1* in M2-like macrophages obtained from
201 infarcted hearts (Figure 2C), which was confirmed by quantitative reverse transcription-
202 polymerase chain reaction (qRT-PCR) and IHC (Figure 2D–E). The data indicate that M2-like
203 macrophages are a source of Nrg1 after MI.
204

205 **Bone Marrow-Derived Macrophages Attenuate Hydrogen Peroxide (H_2O_2)-Induced**
206 **Apoptosis and Senescence of Cardiac Fibroblasts Via Nrg1 Secretion**

207 We investigated the role of macrophages in regulating senescence and apoptosis of fibroblasts in
208 an *in vitro* coculture model using a Boyden Chamber system in which cells can be independently
209 cultured or genetically analyzed without being mixed together[13, 27] (Figure IIIA in the Data
210 Supplement). Hydrogen peroxide (H_2O_2) was used to induce senescence of fibroblasts (Figure
211 IIIB–C in the Data Supplement). Bone marrow-derived macrophages (BMDMs) that were
212 cocultured with the senescent fibroblasts were of an M2-like macrophage phenotype (Figure
213 IVA–B in the Data Supplement). As observed *in vivo* after MI (Figure 2C–E and Figure 1E),
214 increased expression of *Nrg1* was seen in BMDMs (Figure VA in the Data Supplement) and
215 increased expression of *ErbB2* and *ErbB4* was seen in cardiac fibroblasts (Figure VB–C in the

216 Data Supplement) 48 hours after the start of coculture. Phase-contrast microscopy (Figure 3A)
217 showed that fibroblasts treated with H_2O_2 had an enlarged, flattened, senescent morphology, but
218 after coculture with BMDMs the fibroblasts took on a healthy, spindle-shaped form. Importantly,
219 addition of anti-ErbB antibody (Ab), which is a competitive inhibitor of Nrg1, changed the gross
220 morphology of fibroblasts such that they resembled the fibroblasts treated with H_2O_2. Treatment
221 with recombinant Nrg1 restored the senescent fibroblasts to a healthy spindle-shaped form.
222 Approximately 20% of fibroblasts treated with H_2O_2 were found to be positive for senescence-
223 associated β-galactosidase (SA-β-gal) (Figure 3B). This change was significantly attenuated by
224 coculture with BMDMs, whereas addition of anti-ErbB Ab eliminated the anti-senescence effect
225 of the BMDMs. Furthermore, treatment with recombinant Nrg1 suppressed senescence.
226 Expression of apoptosis-related cleaved caspase 3 (Figure 3C) was similar to that of SA-β-gal.
227 Conversely, expression of proliferation-related Ki-67 was significantly attenuated by H_2O_2
228 treatment and restored by co-culture with BMDMs. Effects of the BMDMs were diminished by
229 anti-ErbB Ab, whereas recombinant Nrg1 improved H_2O_2-induced functional deterioration.
230 Together, these results show that Nrg1 derived from BMDMs reduces both apoptosis and
231 senescence of cultured fibroblasts and promotes their proliferation.
232
233 **BMDMs Promote Activation of Fibroblasts and Collagen Synthesis**
234 Immunocytological staining showed that, although treatment with H_2O_2 alone did not affect
235 conversion of cardiac fibroblasts into αSMA^+ myofibroblasts, the phenotypic change progressed
236 in coculture of cardiac fibroblasts with BMDMs. Furthermore, addition of anti-ErbB Ab
237 enhanced this BMDM-induced activation of fibroblasts. Addition of recombinant Nrg1 did not
238 affect conversion of cardiac fibroblasts (Figure 4A). Changes in synthesis of types I and III

239 collagen in fibroblasts in response to H_2O_2, BMDMs, and recombinant Nrg1 were similar to
240 changes in αSMA expression (Figure 4B–C). These results suggest that BMDMs, which are of
241 an M2-like phenotype (Figure IVA–B in the Data Supplement), induce activation of fibroblasts
242 for conversion to myofibroblasts and progression of collagen synthesis. The important take-away
243 point to be drawn from these results is that that cellular senescence and apoptosis alone do not
244 induce activation of fibroblasts for conversion to myofibroblasts and progression of collagen
245 synthesis; the presence of BMDMs is required. Osteopontin (secreted phosphoprotein 1 [SPP1])
246 is a major mediator of M2-like macrophage-induced cardiac fibroblast activation.[13] *Spp1*
247 expression was found to be increased in BMDMs in response to H_2O_2 (Figure VIA in the Data
248 Supplement). Conversely, other profibrotic factors, including transforming growth factor beta
249 and platelet derived growth factor subunit A,[28, 29] were found not to be upregulated in M2-like
250 macrophages (Figure VIB in the Data Supplement).
251
252 **Phosphatidylinositol 3-Kinase/Protein Kinase B Signaling is Associated with BMDM-**
253 **Attenuated Apoptosis and Senescence of Cardiac Fibroblasts Through Nrg1**
254 We next investigated the molecular mechanism underlying attenuation of apoptosis and
255 senescence of cardiac fibroblasts by BMDM-derived Nrg1 in an *in vitro* setting. The
256 phosphatidylinositol 3-kinase (PI3K)/protein kinase B (Akt) signaling pathway is downstream of
257 the ErbB pathway. Western blot analysis showed that H_2O_2 treatment suppressed PI3K/Akt
258 activation in fibroblasts (Figure 5A). Coculture with BMDMs and treatment with recombinant
259 Nrg1upregulated the signaling activity, whereas addition of anti-ErbB Ab suppressed the
260 signaling activity. To determine the possible relation between senescence-associated p21/p16 and
261 Nrg1/ErbB/PI3K/Akt signaling pathways, we examined mRNA expression levels of senescence-

262 associated genes (*p21*, *p16*, and *Glb1)* (Figure 5B), cell cycle-associated genes (cyclin-dependent
263 kinase 4 [*Cdk4*], cyclin-dependent kinase 6 [*Cdk6*], cyclin-dependent kinase 2 [*Cdk2*], and *Ki-*
264 *67*) (Figure 5C), a p53 suppressor gene (murine double minute 2 [*MDM2*]) (Figure 5D), a cell
265 survival-associated gene (mechanistic target of rapamycin [*mTOR*]) (Figure 5E), and an SASP-
266 associated gene (interleukin-6 [*IL-6*]) (Figure 5F). Expression levels of senescence-associated
267 genes (*p16* and *p21*) and the SASP-associated gene (*IL-6*) were significantly higher and
268 expression levels of cell cycle-associated genes (*Cdk4*, *Cdk6*, *Cdk2*, and *Ki-67*) were markedly
269 lower in fibroblasts treated with H_2O_2 than in non-treated (control) fibroblasts. Importantly, these
270 changes in expression were reversed by coculture with BMDMs. Anti-ErbB Ab exacerbated
271 senescence and cell cycle arrest, whereas recombinant Nrg1 suppressed senescence and
272 enhanced proliferation. BMDMs enhanced or restored expression of p53 suppressor-related
273 *MDM2* and cell survival-related *mTOR*. These results indicate that the PI3K/Akt signaling
274 pathway activation in cardiac fibroblasts operates downstream of the BMDM-derived Nrg1/ErbB
275 system and has a suppressive effect on cell cycle arrest and senescence. This signaling activity is
276 also likely to increase cell proliferation and survival (Figure 5G).
277
278 **In Vivo Inhibition of Nrg1 Signaling Exacerbates Fibrosis**
279 We used trastuzumab to clarify the role of Nrg1 in suppressing post-MI senescence and apoptosis
280 of cardiac fibroblasts *in vivo*. Trastuzumab is an anti-ErbB type 2 (ErbB2) monoclonal Ab that
281 binds to the extracellular juxtamembrane domain of ErbB2.[30, 31] On the basis of the *in vitro*
282 coculture model, we hypothesized that trastuzumab administration would eliminate the anti-
283 apoptotic and anti-senescence effects of Nrg1 and therefore allow senescence of cardiac
284 fibroblasts to proceed, which would result in excessive fibrosis in the infarcted myocardium.

285 Intraperitoneal trastuzumab injections did not affect mRNA expression levels of genes associated
286 with senescence, the SASP, or activation of fibroblasts to myofibroblasts in the normal mouse
287 heart (Figure VIIA–C in the Data Supplement). We induced MI in mice surgically and then
288 injected either trastuzumab or vehicle intraperitoneally (Figure VIIIA in the Data Supplement).
289 Trastuzumab did not affect post-MI mortality or body weight (Figure VIIIB–C in the Data
290 Supplement). Gene expression profiles in cardiac fibroblasts resident in infarcted myocardium
291 suggested that senescence was augmented by trastuzumab administration in the infarct area
292 (Figure 6A). The changes in gene expression corresponded to increases in the number of
293 senescent cardiac fibroblasts and cardiac cells in the infarct area (Figure 6B–C). Additionally,
294 trastuzumab administration increased the proportion of fibrotic tissue in the infarct area (Figure
295 7A). In fact, the numbers of Thy-1^{+} fibroblasts and αSMA^{+}Thy1^{+} myofibroblasts were increased
296 in association with upregulation of *αSMA*, *Col1a1*, and *Col3a*1 in the infarct area (Figure 7B–C).
297 Considering these *in vitro* experimental results, increased inflammation (Figure 8A) and boosted
298 accumulation of M2-like macrophages (Figure 8B) in this area by ErbB2 blockade may explain
299 the increased fibroblast activation and augmented fibrosis. Interestingly, trastuzumab
300 administration induced expression of apoptosis- and senescence-associated genes even in the
301 remote area (Figure IXA–C in the Data Supplement) where there was little or no direct ischemic
302 damage after the MI. This corresponded to the increased inflammation (Figure XA in the Data
303 Supplement) and the augmented accumulation of both M2-like macrophages and cardiac
304 fibroblasts in the remote myocardium (Figure XB and Figure XIA in the Data Supplement).
305 Conversion of fibroblasts to myofibroblasts and expression of fibrosis-associated genes were
306 also induced (Figure XI–B in the Data Supplement). Consequently, acute exacerbation of fibrosis
307 occurred even in the remote area (Figure XII in the Data Supplement). Thus, administration of

308 trastuzumab augmented apoptosis and senescence of cardiac fibroblasts following MI, resulting
309 in excessive fibrosis, even in the remote non-infarct area.
310
311 **DISCUSSION**
312 Despite the clinical importance of cellular and molecular processes underlying post-MI fibrosis,
313 the processes are not well understood. To precisely determine the roles of cardiac M2-like
314 macrophages in apoptosis and senescence of fibroblasts, we established an *in vitro* model in
315 which senescent cardiac fibroblasts[32] were cocultured with BMDMs. This *in vitro* coculture
316 model reflects the *in vivo* post-MI conditions because, under pathological conditions, senescent
317 cells attract macrophages.[33] Expression of both *Cdk4/6* and *Cdk2* should be stable or increased in
318 senescent cells, but expression levels were decreased in the cardiac fibroblasts in which
319 senescence was induced by H_2O_2. The mechanism is expected to involve increased expression of
320 *p16* and *p21*, which downregulate *Cdk4/6* and *Cdk2* expression, respectively.[8, 34, 35] Conversely,
321 the addition of BMDMs decreased *p16* and *p21* expression and promoted the cell cycle (as
322 evidenced by increased expression of *Cdk 4/6* and *Cdk2*). The hypertrophic response to Nrg1 is
323 mainly dependent on Ras, whereas the anti-apoptotic and cell proliferation effects are likely
324 dependent on Akt.[36, 37] Therefore, Nrg1 may attenuate expression of senescence-associated genes
325 *p21*, *p16*, and *Glb1* through PI3K/Akt pathways (Figure 5G). We observed a transient increase in
326 *p21*, *p16*, and *Glb1* expression in the infarcted myocardium and in cultured fibroblasts. Stress-
327 induced *p53* expression increases *p21* expression in response to DNA damage and induces
328 reversible proliferative arrest that provides time for DNA repair and facilitates survival of cells.[38,
329 39] p21, which binds to and inhibits CDK2, is important for initiation of senescence in some
330 settings, but *p21* expression does not persist in senescent cells.[8, 34, 40, 41] Increased *p16* expression

331 is found in infarcted tissue. Irreversible proliferative arrest can be induced by p16, which inhibits
332 CDK4 and CDK6.[8, 35] Therefore, the change in expression levels of these genes (i.e., *p21* and
333 *p16*) in both the *in vivo* and *in vitro* experiments suggests that Nrg1 is a crucial factor that
334 controls reversible and irreversible senescence of cardiac cells after MI. Another possible
335 mechanism for the temporal change in *p21* and *p16* expression in the *in vivo* experiment is as
336 follows: There could be multiple types of *p21*- and *p16*-positive cells. Therefore, whereas some
337 *p21*- and *p16*-positive cell populations disappear, other *p21*- and *p16*-positive cells may remain.
338 We showed a possible mechanism linking M2-like macrophages and cardiac fibroblasts, which
339 contributes to various processes that are critical to many aspects of cellular function, including
340 cell growth and survival.[42] Together, results of our *in vivo* and *in vitro* experiments suggest that
341 macrophage-derived Nrg1 suppresses senescence and promotes proliferation of cardiac
342 fibroblasts after myocardial injury by activating the ErbB/PI3K/Akt signaling pathway.
343 ErbB is expressed not only on the surface of fibroblasts but also on the surface of
344 macrophages, and myeloid-specific *ErbB* deletion exacerbates myocardial fibrosis.[21]
345 Furthermore, Nrg1-induced macrophage polarization from an inflammatory phenotype toward an
346 anti-inflammatory phenotype enhances cardiac repair after MI.[22] Therefore, the question was
347 raised whether ErbB signaling in BMDMs was simultaneously affected when anti-ErbB Ab was
348 added to the culture medium in our coculture experiments. The exacerbated phenotypic changes
349 characterizing senescence and apoptosis of fibroblasts might not be due to inhibition of
350 Nrg1/ErbB signaling in the fibroblasts. However, we showed that the phenotypic changes and
351 expression of genes denoting the senescence and apoptosis of H_2O_2-treated cells, with the
352 Nrg1/ErbB signaling-induced activation of BMDMs having been excluded, were similar to those
353 in the H_2O_2+BMDM+anti-ErbB Ab treated cells (Figure 3A–C and Figure 5B–C). Therefore, our

354 data suggest that Nrg1/ErbB signaling activity has a greater anti-senescence and anti-apoptotic
355 effect in fibroblasts than does the signaling activity related to macrophage polarization.
356 Nrg1 is a cytokine that belongs to a family of proteins structurally related to epidermal growth
357 factor, and it plays essential roles in protection and proliferation of cardiomyocytes in response
358 to injury.[16-19] Injecting Nrg1 into adult mice induces cardiomyocyte cell cycle activity and
359 promotes myocardial regeneration, leading to improved function after MI.[16, 18] Nrg1 also
360 significantly decreases apoptosis of adult cardiomyocytes under hypoxia-reoxygenation
361 conditions.[17] However, its function in cardiac fibroblasts in this context has not been well
362 studied. We present new *in vivo* and *in vitro* evidence suggesting that M2-like macrophages play
363 a vital role in attenuating senescence and apoptosis of fibroblasts through Nrg1/ErbB/PI3K/Akt
364 signaling pathways. This inherent reparative function allows senescent cardiac fibroblasts to
365 recover to a certain degree. Conversely, incomplete rescue of fibroblasts from senescence might
366 lead to undesired fibrosis.
367 Previous studies have shown that trastuzumab efficiently stops or slows the growth of ErbB2^{+}
368 cells *in vitro* and inhibits the ability of cells to repair damaged DNA.[30, 31] As inflammation
369 worsens after MI, M2-like macrophages from bone marrow accumulate at the site of damaged
370 tissue.[43] Our study showed that progression of senescence and apoptosis in cardiac fibroblasts
371 and exacerbation of inflammation induced by trastuzumab increased the accumulation of M2-
372 like macrophages, which in turn promoted activation of fibroblasts and excessive fibrosis. These
373 results are consistent with our previous report indicating that interleukin 4-mediated M2-like
374 macrophage activation induces conversion of fibroblasts into myofibroblasts for progression of
375 fibrosis.[13] Although we analyzed mRNA expression levels in sections of heart tissue and not in
376 single cells, increased expression levels of senescence-associated genes in the trastuzumab-

377 treated samples were considered to reflect progression of senescence. These results corresponded
378 to results obtained *in vitro* with use of anti-ErbB Ab. We administered trastuzumab systemically,
379 which has unclarified cardiotoxicity, to explore ErbB signaling in cardiac fibroblasts. Because
380 cardiotoxicity of trastuzumab is non-specific, our study was limited by the fact that the ErbB
381 receptor block achieved with anti-ErbB Ab is not specific to cardiac fibroblasts. Moreover, M2-
382 like macrophages are not the only source of Nrg1 after MI. Apart from the M2-like macrophages
383 we studied, endothelial cells have been identified as a potential cell type for neuregulin
384 production and are responsible for the healing response after myocardial injury.[16-19] Therefore,
385 further mechanistic studies are needed to clarify the signaling pathways downstream of these
386 factors and the clear role of Nrg1, i.e., studies that incorporate cardiac fibroblast-specific
387 conditional *ErbB2/ErbB4*-knockout mice and macrophage-specific conditional *Nrg1*-knockout
388 mice.

389 Interestingly, senescence and SASP-associated gene expression peaked a little later in the
390 remote area than in the infarct area. One possible pathological mechanism of the remote non-
391 infarct area is assumed to be indirect damage via SASP rather than direct cytotoxicity due to
392 ischemia. Senescent cells autonomously induce senescence-like gene expression in surrounding
393 non-senescent cells through the SASP.[44] Increased release of SASP-associated substances in the
394 infarct area might not simply induce senescence and apoptosis of cells in the infarct area; it
395 might also have a harmful influence on non-senescent cells in the remote non-infarct area.

396 Although this study focused on Nrg1-induced anti-apoptosis and anti-senescence of cardiac
397 fibroblasts, M2-like macrophages are likely to mediate supplementary benefits for cardiac repair
398 after MI. These benefits may include reduced inflammation, activation of fibroblasts, and
399 neovascularization, as shown in our previous study.[13] To develop potential therapies mediated by

400 M2-like macrophages, studies are needed to determine how the gene that encodes Nrg1 is
401 switched on by MI and to identify other molecules that regulate apoptosis, senescence, and
402 proliferation of cardiac fibroblasts.
403 In conclusion, our data provide evidence that the Nrg1/ErbB/PI3K/Akt signaling system
404 regulates senescence and apoptosis of cardiac fibroblasts in the infarcted adult murine heart. This
405 process might play a vital role in repair of the infarcted myocardium by regulating collagen
406 synthesis. Therefore, this tissue repair mechanism controls the degree of rigidity and contraction
407 of the infarcted heart, thereby determining the prognosis of MI. Better understanding of the
408 molecular mechanism at play in the healing process of MI and subsequent remodeling may
409 ultimately lead to new treatments. Targeted activation of M2-like macrophages might enhance
410 the endogenous repair mechanism in senescent cardiac fibroblasts and serve as an approach to
411 treatment for MI.
412

413 **Acknowledgments**

414 MS and KS conceived and designed the study. MS conducted most of the experiments and
415 acquired the data with support from AY and KS. All authors participated in the analysis and
416 interpretation of the data. MS and KS primarily wrote and edited the manuscript with input from
417 all other authors. We thank Ellen Knapp, PhD, and Mitchell Arico from Edanz Group (https://en-
418 author-services.edanz.com/ac) for editing a draft of this manuscript. We wish to thank Ms.
419 Wendy Alexander-Adams for her assistance in reporting our findings in English. This project
420 was supported by the Uehara Memorial Foundation, SENSHIN Medical Research Foundation, a
421 Grant-in-Aid for Scientific Research (C), the Mochida Memorial Foundation for Medical and
422 Pharmaceutical Research, Takeda Science Foundation, and Public Trust Surgery Research Fund.

Disclosures

The authors have that no conflicts of interest to disclose.

SUPPLEMENTAL MATERIALS

Extended Methods

Online Figures I–XII

Online Table I–III

432 **References**

433 1. Zhu F, Li Y, Zhang J, Piao C, Liu T, Li HH and Du J. Senescent cardiac fibroblast is
434 critical for cardiac fibrosis after myocardial infarction. *PLoS One*. 2013;8:e74535.
435 2. Dickstein K, Cohen-Solal A, Filippatos G, McMurray JJ, Ponikowski P, Poole-Wilson
436 PA, Stromberg A, van Veldhuisen DJ, Atar D, Hoes AW, Keren A, Mebazaa A, Nieminen M,
437 Priori SG, Swedberg K and Guidelines ESCCfP. ESC Guidelines for the diagnosis and treatment
438 of acute and chronic heart failure 2008: the Task Force for the Diagnosis and Treatment of Acute
439 and Chronic Heart Failure 2008 of the European Society of Cardiology. Developed in
440 collaboration with the Heart Failure Association of the ESC (HFA) and endorsed by the
441 European Society of Intensive Care Medicine (ESICM). *Eur Heart J*. 2008;29:2388-442.
442 3. Gemberling M, Karra R, Dickson AL and Poss KD. Nrg1 is an injury-induced
443 cardiomyocyte mitogen for the endogenous heart regeneration program in zebrafish. *Elife*.
444 2015;4.
445 4. Gould KE, Taffet GE, Michael LH, Christie RM, Konkol DL, Pocius JS, Zachariah JP,
446 Chaupin DF, Daniel SL, Sandusky GE, Jr., Hartley CJ and Entman ML. Heart failure and greater
447 infarct expansion in middle-aged mice: a relevant model for postinfarction failure. *Am J Physiol*
448 *Heart Circ Physiol*. 2002;282:H615-21.
449 5. Takemura G, Ohno M, Hayakawa Y, Misao J, Kanoh M, Ohno A, Uno Y, Minatoguchi
450 S, Fujiwara T and Fujiwara H. Role of apoptosis in the disappearance of infiltrated and
451 proliferated interstitial cells after myocardial infarction. *Circ Res*. 1998;82:1130-8.
452 6. Shih H, Lee B, Lee RJ and Boyle AJ. The aging heart and post-infarction left
453 ventricular remodeling. *J Am Coll Cardiol*. 2011;57:9-17.

454 7. Sharpless NE and Sherr CJ. Forging a signature of in vivo senescence. *Nat Rev*
455 *Cancer*. 2015;15:397-408.
456 8. Munoz-Espin D and Serrano M. Cellular senescence: from physiology to pathology.
457 *Nat Rev Mol Cell Biol*. 2014;15:482-96.
458 9. Coppe JP, Desprez PY, Krtolica A and Campisi J. The senescence-associated secretory
459 phenotype: the dark side of tumor suppression. *Annu Rev Pathol*. 2010;5:99-118.
460 10. Alam P, Haile B, Arif M, Pandey R, Rokvic M, Nieman M, Maliken BD, Paul A, Wang
461 YG, Sadayappan S, Ahmed RPH and Kanisicak O. Inhibition of Senescence-Associated Genes
462 Rb1 and Meis2 in Adult Cardiomyocytes Results in Cell Cycle Reentry and Cardiac Repair Post-
463 Myocardial Infarction. *J Am Heart Assoc*. 2019;8:e012089.
464 11. Hayakawa K, Takemura G, Kanoh M, Li Y, Koda M, Kawase Y, Maruyama R, Okada
465 H, Minatoguchi S, Fujiwara T and Fujiwara H. Inhibition of granulation tissue cell apoptosis
466 during the subacute stage of myocardial infarction improves cardiac remodeling and dysfunction
467 at the chronic stage. *Circulation*. 2003;108:104-9.
468 12. Aurora AB, Porrello ER, Tan W, Mahmoud AI, Hill JA, Bassel-Duby R, Sadek HA and
469 Olson EN. Macrophages are required for neonatal heart regeneration. *J Clin Invest*.
470 2014;124:1382-92.
471 13. Shiraishi M, Shintani Y, Shintani Y, Ishida H, Saba R, Yamaguchi A, Adachi H, Yashiro
472 K and Suzuki K. Alternatively activated macrophages determine repair of the infarcted adult
473 murine heart. *J Clin Invest*. 2016;126:2151-66.
474 14. Meyer D, Yamaai T, Garratt A, Riethmacher-Sonnenberg E, Kane D, Theill LE and
475 Birchmeier C. Isoform-specific expression and function of neuregulin. *Development*.
476 1997;124:3575-86.

477 15. Fuller SJ, Sivarajah K and Sugden PH. ErbB receptors, their ligands, and the
478 consequences of their activation and inhibition in the myocardium. *J Mol Cell Cardiol*.
479 2008;44:831-54.
480 16. Bersell K, Arab S, Haring B and Kuhn B. Neuregulin1/ErbB4 signaling induces
481 cardiomyocyte proliferation and repair of heart injury. *Cell*. 2009;138:257-70.
482 17. Hedhli N, Huang Q, Kalinowski A, Palmeri M, Hu X, Russell RR and Russell KS.
483 Endothelium-derived neuregulin protects the heart against ischemic injury. *Circulation*.
484 2011;123:2254-62.
485 18. Polizzotti BD, Ganapathy B, Walsh S, Choudhury S, Ammanamanchi N, Bennett DG,
486 dos Remedios CG, Haubner BJ, Penninger JM and Kuhn B. Neuregulin stimulation of
487 cardiomyocyte regeneration in mice and human myocardium reveals a therapeutic window. *Sci*
488 *Transl Med*. 2015;7:281ra45.
489 19. Lemmens K, Doggen K and De Keulenaer GW. Role of neuregulin-1/ErbB signaling
490 in cardiovascular physiology and disease: implications for therapy of heart failure. *Circulation*.
491 2007;116:954-60.
492 20. Kirabo A, Ryzhov S, Gupte M, Sengsayadeth S, Gumina RJ, Sawyer DB and Galindo
493 CL. Neuregulin-1beta induces proliferation, survival and paracrine signaling in normal human
494 cardiac ventricular fibroblasts. *J Mol Cell Cardiol*. 2017;105:59-69.
495 21. Vermeulen Z, Hervent AS, Dugaucquier L, Vandekerckhove L, Rombouts M, Beyens
496 M, Schrijvers DM, De Meyer GRY, Maudsley S, De Keulenaer GW and Segers VFM. Inhibitory
497 actions of the NRG-1/ErbB4 pathway in macrophages during tissue fibrosis in the heart, skin,
498 and lung. *Am J Physiol Heart Circ Physiol*. 2017;313:H934-H945.

499 22. Pascual-Gil S, Abizanda G, Iglesias E, Garbayo E, Prosper F and Blanco-Prieto MJ.
500 NRG1 PLGA MP locally induce macrophage polarisation toward a regenerative phenotype in the
501 heart after acute myocardial infarction. *J Drug Target*. 2019;27:573-581.
502 23. Krizhanovsky V, Yon M, Dickins RA, Hearn S, Simon J, Miething C, Yee H, Zender L
503 and Lowe SW. Senescence of activated stellate cells limits liver fibrosis. *Cell*. 2008;134:657-67.
504 24. van Deursen JM. The role of senescent cells in ageing. *Nature*. 2014;509:439-46.
505 25. Olayioye MA, Neve RM, Lane HA and Hynes NE. The ErbB signaling network:
506 receptor heterodimerization in development and cancer. *EMBO J*. 2000;19:3159-67.
507 26. Uray IP, Connelly JH, Thomazy V, Shipley GL, Vaughn WK, Frazier OH, Taegtmeyer
508 H and Davies PJ. Left ventricular unloading alters receptor tyrosine kinase expression in the
509 failing human heart. *J Heart Lung Transplant*. 2002;21:771-82.
510 27. Suzuki T, Arumugam P, Sakagami T, Lachmann N, Chalk C, Sallese A, Abe S, Trapnell
511 C, Carey B, Moritz T, Malik P, Lutzko C, Wood RE and Trapnell BC. Pulmonary macrophage
512 transplantation therapy. *Nature*. 2014;514:450-4.
513 28. van den Borne SW, Diez J, Blankesteijn WM, Verjans J, Hofstra L and Narula J.
514 Myocardial remodeling after infarction: the role of myofibroblasts. *Nat Rev Cardiol*. 2010;7:30-
515 7.
516 29. Shinde AV and Frangogiannis NG. Fibroblasts in myocardial infarction: a role in
517 inflammation and repair. *J Mol Cell Cardiol*. 2014;70:74-82.
518 30. Park S, Jiang Z, Mortenson ED, Deng L, Radkevich-Brown O, Yang X, Sattar H, Wang
519 Y, Brown NK, Greene M, Liu Y, Tang J, Wang S and Fu YX. The therapeutic effect of anti-
520 HER2/neu antibody depends on both innate and adaptive immunity. *Cancer Cell*. 2010;18:160-
521 70.

522 31. ElZarrad MK, Mukhopadhyay P, Mohan N, Hao E, Dokmanovic M, Hirsch DS, Shen
523 Y, Pacher P and Wu WJ. Trastuzumab alters the expression of genes essential for cardiac function
524 and induces ultrastructural changes of cardiomyocytes in mice. *PLoS One*. 2013;8:e79543.
525 32. Bladier C, Wolvetang EJ, Hutchinson P, de Haan JB and Kola I. Response of a primary
526 human fibroblast cell line to H2O2: senescence-like growth arrest or apoptosis? *Cell Growth*
527 *Differ*. 1997;8:589-98.
528 33. Sasaki M, Miyakoshi M, Sato Y and Nakanuma Y. Modulation of the
529 microenvironment by senescent biliary epithelial cells may be involved in the pathogenesis of
530 primary biliary cirrhosis. *J Hepatol*. 2010;53:318-25.
531 34. Childs BG, Durik M, Baker DJ and van Deursen JM. Cellular senescence in aging and
532 age-related disease: from mechanisms to therapy. *Nat Med*. 2015;21:1424-35.
533 35. Serrano M, Lin AW, McCurrach ME, Beach D and Lowe SW. Oncogenic ras provokes
534 premature cell senescence associated with accumulation of p53 and p16INK4a. *Cell*.
535 1997;88:593-602.
536 36. Kuramochi Y, Cote GM, Guo X, Lebrasseur NK, Cui L, Liao R and Sawyer DB.
537 Cardiac endothelial cells regulate reactive oxygen species-induced cardiomyocyte apoptosis
538 through neuregulin-1beta/erbB4 signaling. *J Biol Chem*. 2004;279:51141-7.
539 37. Baliga RR, Pimental DR, Zhao YY, Simmons WW, Marchionni MA, Sawyer DB and
540 Kelly RA. NRG-1-induced cardiomyocyte hypertrophy. Role of PI-3-kinase, p70(S6K), and
541 MEK-MAPK-RSK. *Am J Physiol*. 1999;277:H2026-37.
542 38. Deng C, Zhang P, Harper JW, Elledge SJ and Leder P. Mice lacking p21CIP1/WAF1
543 undergo normal development, but are defective in G1 checkpoint control. *Cell*. 1995;82:675-84.

544 39. Wang YA, Elson A and Leder P. Loss of p21 increases sensitivity to ionizing radiation
545 and delays the onset of lymphoma in atm-deficient mice. *Proc Natl Acad Sci U S A*.
546 1997;94:14590-5.
547 40. Alcorta DA, Xiong Y, Phelps D, Hannon G, Beach D and Barrett JC. Involvement of
548 the cyclin-dependent kinase inhibitor p16 (INK4a) in replicative senescence of normal human
549 fibroblasts. *Proc Natl Acad Sci U S A*. 1996;93:13742-7.
550 41. Stein GH, Drullinger LF, Soulard A and Dulic V. Differential roles for cyclin-
551 dependent kinase inhibitors p21 and p16 in the mechanisms of senescence and differentiation in
552 human fibroblasts. *Mol Cell Biol*. 1999;19:2109-17.
553 42. Yu JS and Cui W. Proliferation, survival and metabolism: the role of
554 PI3K/AKT/mTOR signalling in pluripotency and cell fate determination. *Development*.
555 2016;143:3050-60.
556 43. Ikeda N, Asano K, Kikuchi K, Uchida Y, Ikegami H, Takagi R, Yotsumoto S, Shibuya
557 T, Makino-Okamura C, Fukuyama H, Watanabe T, Ohmuraya M, Araki K, Nishitai G and Tanaka
558 M. Emergence of immunoregulatory Ym1(+)Ly6C(hi) monocytes during recovery phase of
559 tissue injury. *Sci Immunol*. 2018;3.
560 44. Acosta JC, Banito A, Wuestefeld T, Georgilis A, Janich P, Morton JP, Athineos D,
561 Kang TW, Lasitschka F, Andrulis M, Pascual G, Morris KJ, Khan S, Jin H, Dharmalingam G,
562 Snijders AP, Carroll T, Capper D, Pritchard C, Inman GJ, Longerich T, Sansom OJ, Benitah SA,
563 Zender L and Gil J. A complex secretory program orchestrated by the inflammasome controls
564 paracrine senescence. *Nat Cell Biol*. 2013;15:978-90.
565 45. Tano N, Narita T, Kaneko M, Ikebe C, Coppen SR, Campbell NG, Shiraishi M,
566 Shintani Y and Suzuki K. Epicardial placement of mesenchymal stromal cell-sheets for the

567 treatment of ischemic cardiomyopathy; in vivo proof-of-concept study. *Mol Ther*. 2014;22:1864-
568 71.
569 46. Leicht M, Greipel N and Zimmer H. Comitogenic effect of catecholamines on rat
570 cardiac fibroblasts in culture. *Cardiovasc Res*. 2000;48:274-84.
571 47. Shintani Y, Kapoor A, Kaneko M, Smolenski RT, D'Acquisto F, Coppen SR, Harada-
572 Shoji N, Lee HJ, Thiemermann C, Takashima S, Yashiro K and Suzuki K. TLR9 mediates
573 cellular protection by modulating energy metabolism in cardiomyocytes and neurons. *Proc Natl*
574 *Acad Sci U S A*. 2013;110:5109-14.
575

576 **Figure legends**

577

578 **Figure 1. Myocardial infarction (MI) induces apoptosis and senescence of cardiac**

579 **fibroblasts and upregulates Nrg1 expression in infarcted myocardium.**

580 **A**, Double immunofluorescence staining for Thy1 and cleaved caspase 3 (CC3), performed on

581 post-MI days 7 and 28, revealed a significantly increased number of apoptotic cardiac

582 fibroblasts in the infarct area, relative to the number seen in the remote area. Scale bars: 100

583 μm. *n*=4 samples each.

584 **B**, Staining for senescence-associated beta-galactosidase (SA-β-gal) on post-MI days 7 and 28

585 revealed a significantly increased accumulation of spindle-shaped senescent cells in the

586 infarct area relative to that in the remote area. Scale bars: 100 μm.

587 **C**, Quantitative reverse transcription-polymerase chain reaction (qRT-PCR) revealed significant

588 upregulation of senescence-associated genes (*p16* and *Glb1*) in the infarct area on post-MI

589 day 7 or 28 or both. *n*=4 samples each.

590 **D**, qRT-PCR analysis confirmed significant upregulation of *Nrg1* in the infarct area on post-MI

591 day 7. *n*=4 samples each.

592 **E**, On immunohistochemistry, the $Thy1^{+}ErbB2^{+}$ fibroblast/$Thy1^{+}$ fibroblast ratio and the

593 $Thy1^{+}ErbB4^{+}$ fibroblast/$Thy1^{+}$ fibroblast ratio determined on post-MI day 7 and 28 were

594 found to be significantly increased. Scale bars: 100 μm. *n*=4 samples each. Gene expression

595 levels relative to those in non-MI heart (Day 0) are given. Mean±SEM values are shown

596 $^{*}P<0.05$, $^{**}P<0.01$, $^{***}P<0.005$ versus the remote area; $^{\#}P<0.05$, $^{\#\#}P<0.01$, $^{\#\#\#}P<0.005$

597 versus non-MI heart; 1-way ANOVA.

598

599 **Figure 2. M2-like macrophages accumulate in the infarct area and express Nrg1.**

600 **A**, Immunohistochemistry revealed increased accumulation of $CD206^+$ M2-like macrophages in

601 the infarct area, which peaked on post-MI day 7. Scale bars: 100 μm. n=4 samples each.

602 Mean±SEM values are shown.

603 *P<0.05, **P<0.01, ***P<0.005 versus the remote area; $^{\#}P$<0.05, $^{\#\#}P$<0.01, $^{\#\#\#}P$<0.005

604 versus non-MI heart; 1-way ANOVA.

605 **B**, Flow cytometric analysis confirmed the presence of $CD206^+F4/80^+CD11b^+$ M2-like

606 macrophages in normal (non-MI) hearts of adult C57BL/6 mice and in hearts of mice

607 subjected to MI. n=6 samples each.

608 **C**, Microarray analysis showed the M2 macrophages after MI to have a different expression

609 profile from that of M2 macrophages in hearts not subjected to MI. The scatter plot shows

610 upregulation of 70 genes and downregulated of 39 genes in M2-like macrophages after MI

611 compared to M2-like macrophages . Among the upregulated genes is neuregulin 1 (*Nrg1*).

612 **D**, Quantitative reverse transcription-polymerase chain reaction confirmed post-MI upregulation

613 of *Nrg1* in $CD206^+F4/80^+CD11b^+$ cardiac M2-like macrophages after MI. n=4 samples each.

614 Gene expression levels relative to those in M2-like macrophages from normal hearts are

615 shown. Mean±SEM values are shown.

616 $^{\#}P$<0.05, $^{\#\#}P$<0.01, $^{\#\#\#}P$<0.005 versus M2-like macrophages from normal hearts, 2-tailed,

617 unpaired Student's t-test.

618 **E**, Double immunofluorescence staining revealed Nrg1 expression on the surface of $CD206^+$

619 M2-like macrophages. Scale bars: 100 μm. n=4 samples each.

620

621 **Figure 3. Bone marrow-derived macrophages (BMDMs) attenuate H_2O_2-induced apoptosis**
622 **and senescence of cardiac fibroblasts via Nrg1 secretion.**
623 **A,** Representative phase-contrast microscopy images. Treatment with a hydrogen peroxide
624 (H_2O_2) solution changed the spindle-shaped appearance of cardiac fibroblasts to a
625 significantly enlarged, flattened morphology. Addition of bone marrow-derived macrophages
626 (BMDMs) altered the senescent morphology to a normal, spindle-shaped morphology. After
627 addition of anti-ErbB antibody (Ab), fibroblasts displayed the same gross morphology as that
628 of senescent fibroblasts treated with H_2O_2. Likewise, addition of recombinant neuregulin 1
629 (Nrg1) changed the gross morphology to a spindle shape. Scale bars: 100 μm. *n*=4 samples
630 each.
631 **B**. Staining for SA-β-gal showed that senescence was exacerbated in H_2O_2-treated fibroblasts but
632 not in fibroblasts cocultured with BMDMs. This suppression of senescence was attenuated by
633 coculture with the anti-ErbB Ab. Nrg1 suppressed fibroblast senescence. Scale bars: 100 μm.
634 *n*=4 samples each.
635 **C**. Apoptosis of cardiac fibroblasts (ratio of cleaved caspase 3^+DAPI$^+$ fibroblasts to DAPI$^+$
636 fibroblasts) was increased in coculture with H_2O_2 but decreased in coculture with BMDMs.
637 This decrease in apoptosis was eliminated by the anti-ErbB Ab. Nrg1 suppressed apoptosis.
638 Nuclei were counterstained with 4′,6-diamidino-2-phenylindole (DAPI). *n*=4 samples each.
639 Scale bars: 100 μm.
640 **D**, Proliferation of cardiac fibroblasts (ratio of Ki-67$^+$ and DAPI$^+$ fibroblasts to DAPI$^+$
641 fibroblasts) was decreased under H_2O_2 treatment but increased when cells were cocultured
642 with BMDMs. This enhanced proliferation was suppressed by the anti-ErbB Ab. Nrg1

643 accelerated proliferation. Nuclei were counterstained with DAPI. Scale bars: 50 μm. *n*=4

644 samples each. Mean±SEM values are shown.

645 $^{\#}P<0.05$ versus normal cardiac fibroblasts (control), $^{*}P<0.05$ versus H_2O_2, $^{\ddagger}P<0.05$ versus

646 H_2O_2+BMDMs, $^{\dagger}P<0.05$ versus H_2O_2+BMDMs+Ab, $^{\S}P<0.05$ versus H_2O_2+Nrg1; 1-way

647 ANOVA.

648

649 **Figure 4. Bone marrow-derived macrophages (BMDMs) promote fibroblast activation and**

650 **collagen synthesis.**

651 **A–C**. Representative images of cardiac fibroblasts stained immunocytochemically for (A)

652 vimentin and αSMA, (B) vimentin and collagen I, and (C) vimentin and collagen III. The

653 staining was performed 48 hours after the start of culture.

654 **A,** Activation of cardiac fibroblasts (ratio of vimentin^{+} and αSMA^{+} myofibroblasts to vimentin^{+}

655 fibroblasts) was equal under treatment with hydrogen peroxide (H_2O_2) but markedly

656 increased when cells were cocultured with bone marrow-derived macrophages (BMDMs).

657 This increase in activation was accelerated by the anti-ErbB antibody (Ab). Addition of

658 recombinant neuregulin 1 (Nrg1) did not affect activation. Scale bars: 100 μm. *n*=4 samples

659 each.

660 **B**. Collagen I synthesis was equal under treatment with H_2O_2 but significantly increased when

661 cells were cocultured with BMDMs. This increase in production was enhanced by treatment

662 with anti-ErbB Ab. Addition of Nrg1 did not affect collagen I synthesis. Scale bars: 100 μm.

663 *n*=4 samples each.

664 **C**. Collagen III synthesis was similar to collagen I synthesis. Scale bars: 100 μm. *n*=4 samples

665 each. Mean±SEM values are shown.

666 $^{\#}P<0.05$ versus normal cardiac fibroblasts (control), $^{*}P<0.05$ versus H_2O_2, $^{\ddagger}P<0.05$ versus
667 H_2O_2+BMDMs, $^{\dagger}P<0.05$ versus H_2O_2+BMDMs+Ab, $^{\S}P<0.05$ versus H_2O_2+Nrg1; 1-way
668 ANOVA.
669
670 **Figure 5.** ***PI3K/Akt signaling pathway is associated with BMDM-attenuated apoptosis and***
671 ***senescence of cardiac fibroblasts through Nrg1.***
672 **A**. Representative bands of PI3K, pPI3K, Akt, pAkt, and β-actin in cardiac fibroblasts treated (or
673 not treated) with hydrogen peroxide (H_2O_2), in those cocultured with bone marrow-derived
674 macrophages (BMDMs), and those treated (or not treated) with anti-ErbB antibody
675 (Ab)/recombinant neuregulin 1 (Nrg1). Treatment and coculture lasted 48 hours. Bar graph
676 shows quantification of relative pPI3k/PI3k and pAkt/Akt. H_2O_2 alone did not affect activation
677 of PI3K/AKT signaling in fibroblasts. Addition of BMDMs significantly activated the signaling
678 pathway and, conversely, addition of the anti-ErbB Ab impaired it. Nrg1 re-stimulated the
679 signaling pathway. n=4 samples each.
680 **B**. Quantitative reverse transcription-polymerase chain reaction analysis of cardiac fibroblasts
681 having been treated (or not) with H_2O_2, co-cultured with BMDMs, and treated (or not) with
682 anti-ErbB Ab/Nrg1. Treatment and coculture lasted 48 hours. Expression levels of
683 senescence-associated genes (*p21, p16*, and *Glb1*) were increased in cells treated with H_2O_2
684 but decreased with the addition of BMDMs. Addition of the anti-ErbB Ab exacerbated
685 senescence and, conversely, addition of Nrg1 suppressed it. n=4 samples each.
686 **C**. Expression of cell cycle-associated genes (*Cdk4*, *Cdk6*, *Cdk2*, and *Ki-67*) were suppressed in
687 cells treated with H_2O_2 but restored in cells cocultured with BMDMs. Addition of anti-ErbB

688 Ab decreased such expression and, conversely, addition of Nrg1 restored such expression.
689 *n*=4 samples each.
690 **D**, Expression of the p53 suppressor gene (*MDM2*) was significantly increased in cells
691 cocultured with BMDMs. *n*=4 samples each.
692 **E**, Expression of cell survival-associated gene (*mTOR*) was suppressed in cells treated with H_2O_2
693 but restored in cells cocultured with BMDMs. Addition of anti-ErbB Ab re-suppressed the
694 expression and, conversely, addition of Nrg1 restored the *mTOR* expression.
695 **F**, Expression of senescence-associated secretory phenotype-associated gene (*IL-6*) was
696 significantly increased in cells treated with H_2O_2 and in those cocultured with BMDMs, with
697 ErbB Ab having been added. *n*=4 samples each.
698 **G**, Schematic representation and overview of the Nrg1/PI3K/AKT pathway. H_2O_2 treatment
699 contributes to the development of cellular damage, which leads to senescence, cell cycle
700 arrest. Nrg1 binding to coreceptor ErbB2/ErbB4 leads to activation of PI3K/AKT and
701 inactivation of p53 and p21, which results in anti-senescence, cell survival and proliferation.
702 Arrowheads indicate stimulation, whereas hammerheads represent inhibition. Gene
703 expression levels relative to the normal cardiac fibroblasts (control) are given. Mean±SEM
704 values are shown.
705 $^{\#}P<0.05$ versus control, $^{*}P<0.05$ versus H_2O_2, $^{\ddagger}P<0.05$ versus H_2O_2+BMDMs, $^{\dagger}P<0.05$
706 versus H_2O_2+BMDMs+Ab, $^{\S}P<0.05$ versus H_2O_2+Nrg1; 1-way ANOVA.
707
708 **Figure 6. In vivo inhibition of Nrg1 signaling promotes apoptosis and senescence of cardiac**
709 **fibroblasts.**

710 **A,** Quantitative reverse transcription-polymerase chain reaction (qRT-PCR) analysis showed
711 post-myocardial infarction (MI) upregulation of senescence-associated genes (*p21*, *p16,* and
712 *Glb1*) in the infarct area after intraperitoneal injection of the mice with trastuzumab in
713 comparison to expression of these genes in vehicle injected post-MI heart. n=4 samples each.
714 **B**, Double immunofluorescence staining of Thy1 and cleaved caspase 3 (CC3) showed the ratio
715 of apoptotic cardiac fibroblasts in the infarct area to be increased on post-MI days 7, 14, and
716 28 in mice injected intraperitoneally with trastuzumab compared with that in mice injected
717 with vehicle only. Arrow shows $Thy1^{+}CC3^{+}$ cells. Scale bars: 100 μm. n=4 samples each.
718 **C**, SA-β-gal staining revealed increased senescence of cardiac cells in the infarct area on post-MI
719 days 7 and 14 after intraperitoneal trastuzumab injection compared with senescence after
720 vehicle injection. Scale bars: 100 μm. n=4 samples each. Gene expression levels relative to
721 levels in non-MI heart (day 0) are given. Mean±SEM values are shown.
722 $^{*}P<0.05$, $^{**}P<0.01$, $^{***}P<0.005$ versus other sample(s); $^{\#}P<0.05$, $^{\#\#}P<0.01$, $^{\#\#\#}P<0.005$
723 versus non-MI heart; 1-way ANOVA.
724
725 **Figure 7. In vivo inhibition of Nrg1 signaling activates cardiac fibroblasts and exacerbates**
726 **fibrosis.**
727 **A,** Masson trichrome staining demonstrated that deposition of collagen fibrils was increased in
728 the infarct area with a time lapse. Intraperitoneal trastuzumab injection significantly increased
729 collagen fibrils in the infarct area. Scale bars: 100 μm. n=4 samples each.
730 **B**, Double immunofluorescence staining of Thy1 and αSMA showed increased accumulation and
731 activation of cardiac fibroblasts in the infarct area following trastuzumab injection versus
732 vehicle injection. Scale bars: 100 μm. n=4 samples each.

733 **C**, Quantitative reverse transcription-polymerase chain reaction (qRT-PCR) analysis showed
734 post-MI upregulation of fibrosis-associated genes (*αSMA*, *Col1a1*, and *Col3a1*) in mice after
735 intraperitoneal trastuzumab injection compared with expression in mice after vehicle
736 injection. n=4 samples each. Gene expression levels relative to levels in non-MI heart (day 0)
737 are given. Mean±SEM values are shown.
738 *P<0.05, **P<0.01, ***P<0.005 versus other sample(s); $^{\#}P$<0.05, $^{\#\#}P$<0.01, $^{\#\#\#}P$<0.005
739 versus the non-MI heart; 1-way ANOVA.
740
741 **Figure 8*. In vivo inhibition of Nrg1 signaling exacerbates myocardial inflammation and***
742 ***promotes accumulation of M2-like macrophages.***
743 **A,** Quantitative reverse transcription-polymerase chain reaction analysis (qRT-PCR) showed
744 post-myocardial infarction (MI) upregulation of senescence-associated secretory phenotype-
745 associated genes (*CCL3*, *IL-6*, and *TNF*) in mice given trastuzumab by intraperitoneal
746 injection compared with expression in vehicle-injected mice. n=4 samples each.
747 **B**, Immunohistochemistry showed intraperitoneal trastuzumab injection significantly accelerated
748 accumulation of CD206^{+} M2-like macrophages in the infarct area with a post-MI peak on day
749 7. Scale bars: 100 μm. n=4 samples each. Gene expression levels relative to levels in non-MI
750 heart (day 0) are given. Mean±SEM values are shown.
751 *P<0.05, **P<0.01, ***P<0.005 versus other sample(s); $^{\#}P$<0.05 $^{\#\#}P$<0.01, $^{\#\#\#}P$<0.005
752 versus non-MI heart; 1-way ANOVA.
753

754 **Novelty And Significance**

755 **What Is Known?**

756 • M2-like macrophages play a role in post-MI fibrotic tissue formation through activation of
757 cardiac fibroblasts.

758 • Nrg1/ErbB signaling systems play essential roles in protection and proliferation of
759 cardiomyocytes in response to injury.

760 • Nrg1/ErbB signaling contributes to macrophage polarization toward an anti-inflammatory
761 phenotype to assist cardiac tissue repair.

762 **What New Information Does This Article Contribute?**

763 • M2-like macrophage-derived Nrg1/ErbB/PI3K/Akt signaling plays a role in suppressing
764 both senescence and apoptosis of cardiac fibroblasts, which greatly affect fibrotic tissue
765 formation in infarcted adult mouse heart.

766

767 M2-like macrophages play an important role in fibrotic tissue formation after myocardial
768 infarction (MI) by activating cardiac fibroblasts. Understanding the effects of apoptosis and
769 senescence on cellular function during tissue repair after MI is important. M2-like macrophages
770 mediate many supplementary benefits in post-MI cardiac repair (e.g., by playing anti-
771 inflammatory and pro-angiogenic roles), in addition to activating cardiac fibroblasts. However,
772 the molecular mechanism by which M2-like macrophages affect the anti-senescence and anti-
773 fibrotic environment after MI has remained unclear. We found that Nrg1, which is known to be
774 expressed by endothelial cells, is also expressed in cardiac $CD206^{+}F4/80^{+}CD11b^{+}$ M2-like
775 macrophages after MI. In the M2-like macrophage and senescent cardiac fibroblast coculture
776 model, M2-like macrophages suppressed senescence and apoptosis of cardiac fibroblasts,

777 whereas blockade of ErbB function significantly accelerated senescence and apoptosis, resulting
778 in increased collagen synthesis. We showed that the molecular mechanism underlying regulation
779 of fibrotic tissue formation in the infarcted myocardium was in part a reduction in apoptosis and
780 senescence of cardiac fibroblasts by activation of Nrg1/ErbB/PI3K/Akt signaling. Furthermore,
781 systemic blockade of ErbB function exacerbated inflammation and increased accumulation of
782 M2-like macrophages, which resulted in excessive progression of fibrosis. Our finding that Nrg1
783 critically regulates senescence and apoptosis of cardiac fibroblasts clarifies a part of the
784 mechanism underlying formation of fibrotic tissue after MI. Targeted activation of M2-like
785 macrophages might enhance this endogenous repair mechanism in senescent and apoptotic
786 cardiac fibroblasts and ultimately provide a new treatment option for MI.
787

Figure 1.

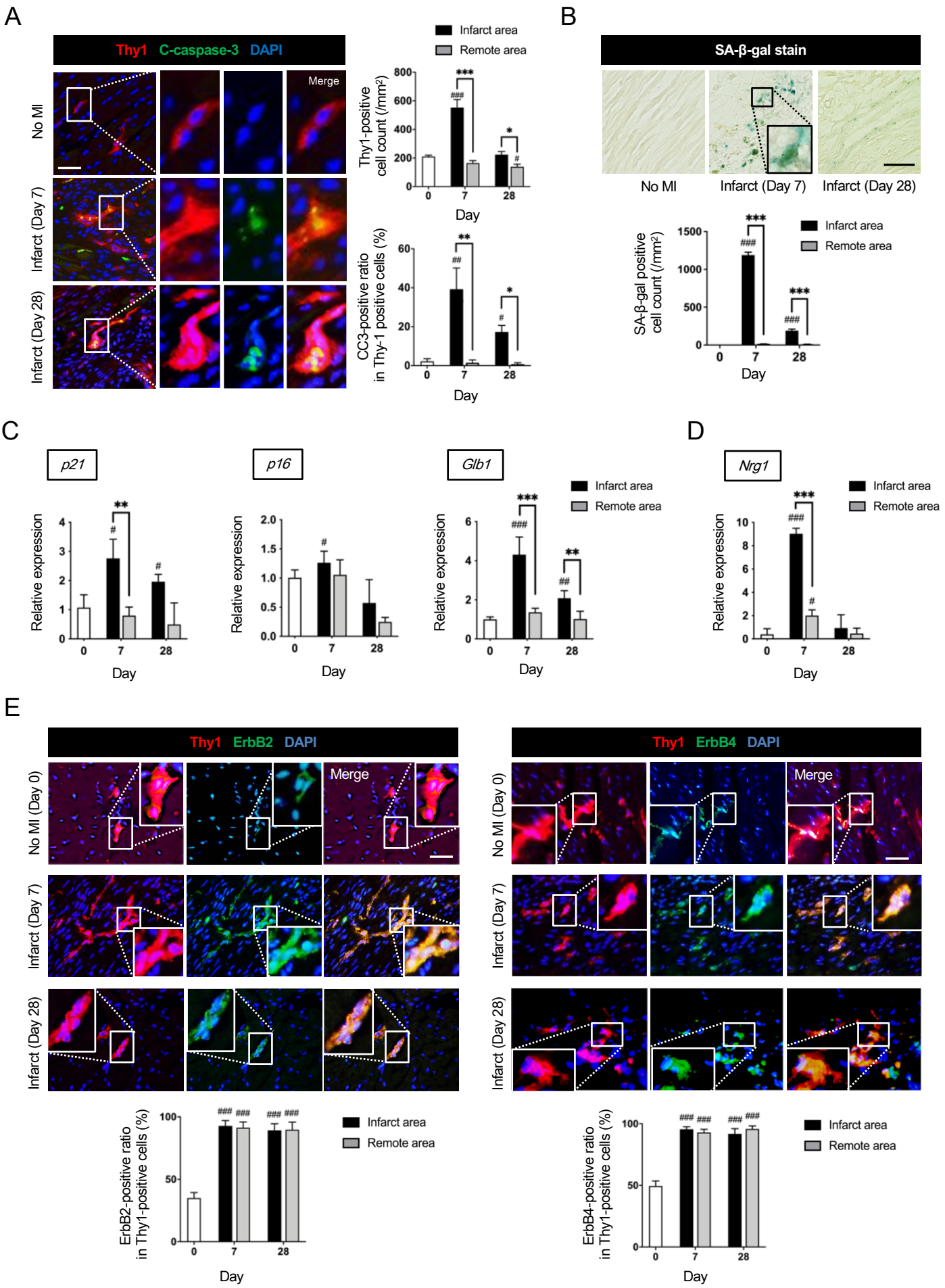
A
Thy1 C-caspase-3 DAPI
Merge
No MI
Infarct (Day 7)
Infarct (Day 28)
Infarct area
Remote area
Thy1-positive cell count (/mm²)
CC3-positive ratio in Thy-1 positive cells (%)
Day
B
SA-β-gal stain
No MI
Infarct (Day 7)
Infarct (Day 28)
SA-β-gal positive cell count (/mm²)
C
p21
p16
Glb1
Relative expression
D
Nrg1
E
Thy1 ErbB2 DAPI
Thy1 ErbB4 DAPI
ErbB2-positive ratio in Thy1-positive cells (%)
ErbB4-positive ratio in Thy1-positive cells (%)

Figure 2.

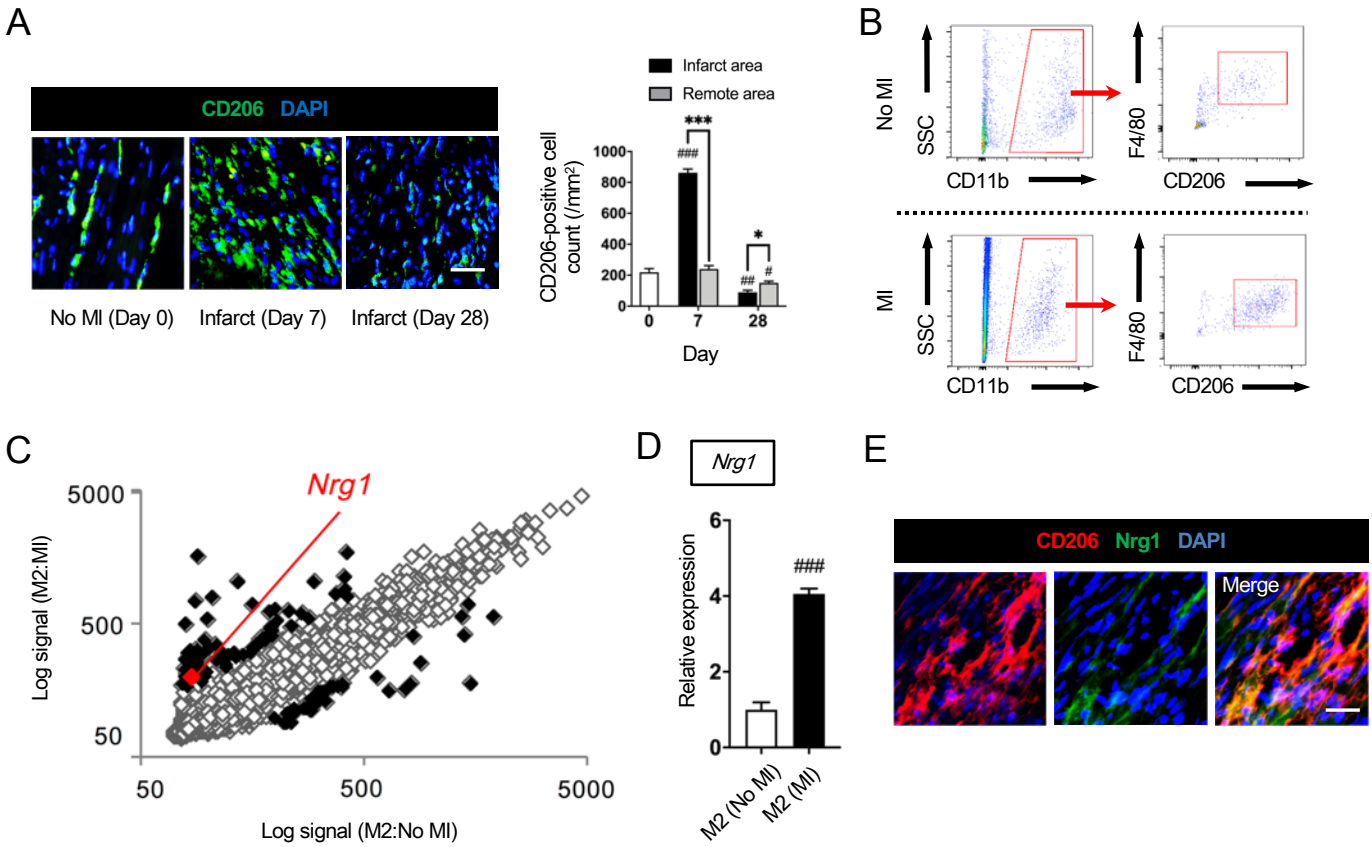
A
CD206 DAPI
No MI (Day 0)
Infarct (Day 7)
Infarct (Day 28)
Infarct area
Remote area
CD206-positive cell count (/mm²)
1000
800
600
400
200
0
***
###
*
##
#
0
7
28
Day
B
No MI
SSC
CD11b
F4/80
CD206
MI
SSC
CD11b
F4/80
CD206
C
Nrg1
5000
500
50
Log signal (M2:MI)
50
500
5000
Log signal (M2:No MI)
D
Nrg1
Relative expression
6
4
2
0
###
M2 (No MI)
M2 (MI)
E
CD206 Nrg1 DAPI
Merge

Figure 3.

A

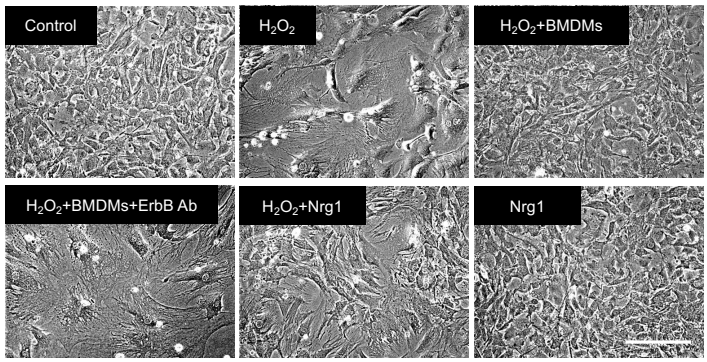

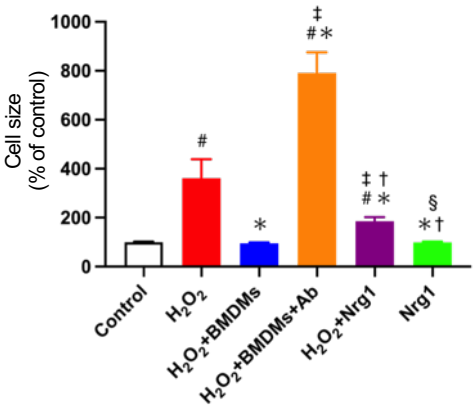

B

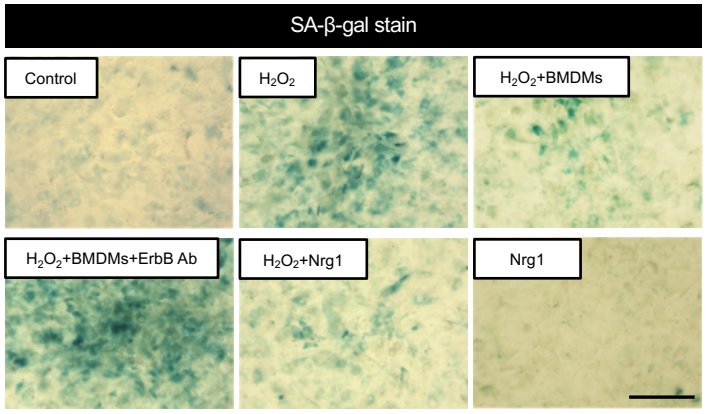

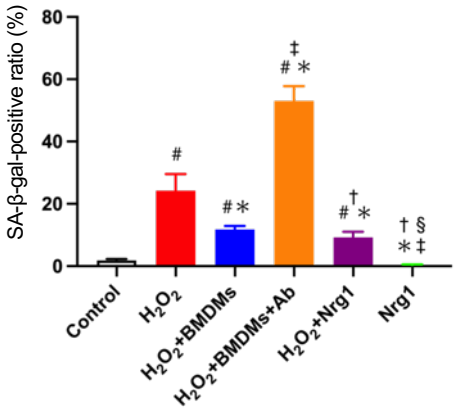

C

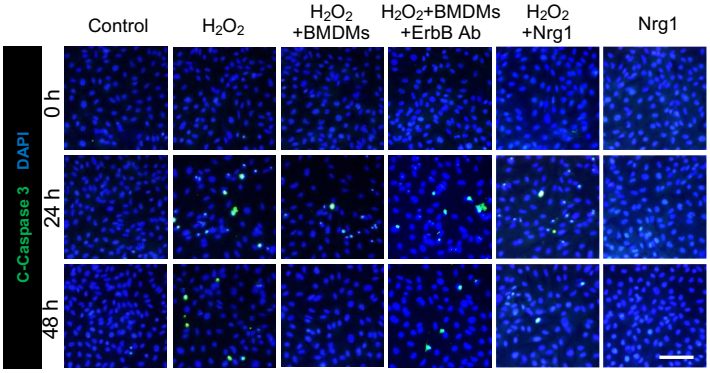

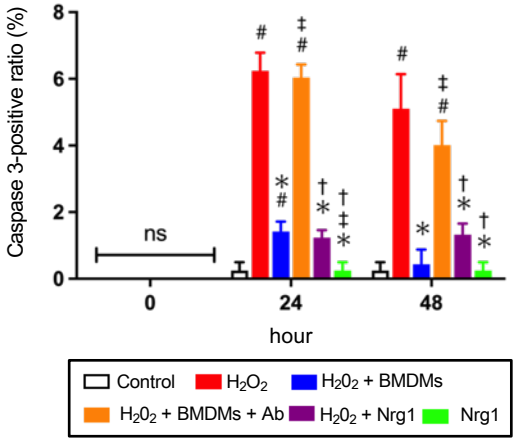

D

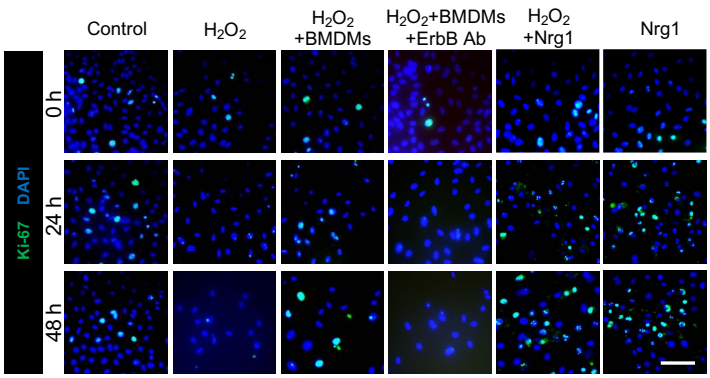

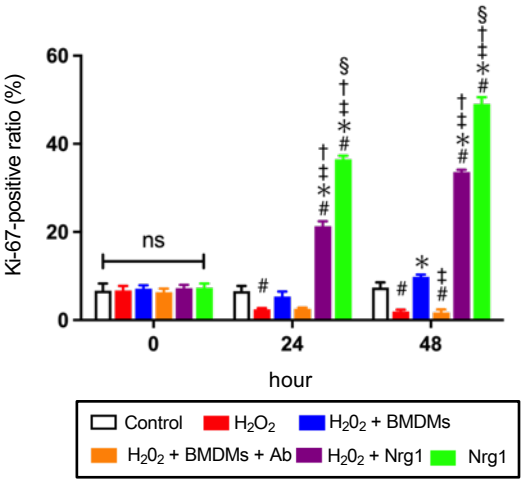

Figure 4.

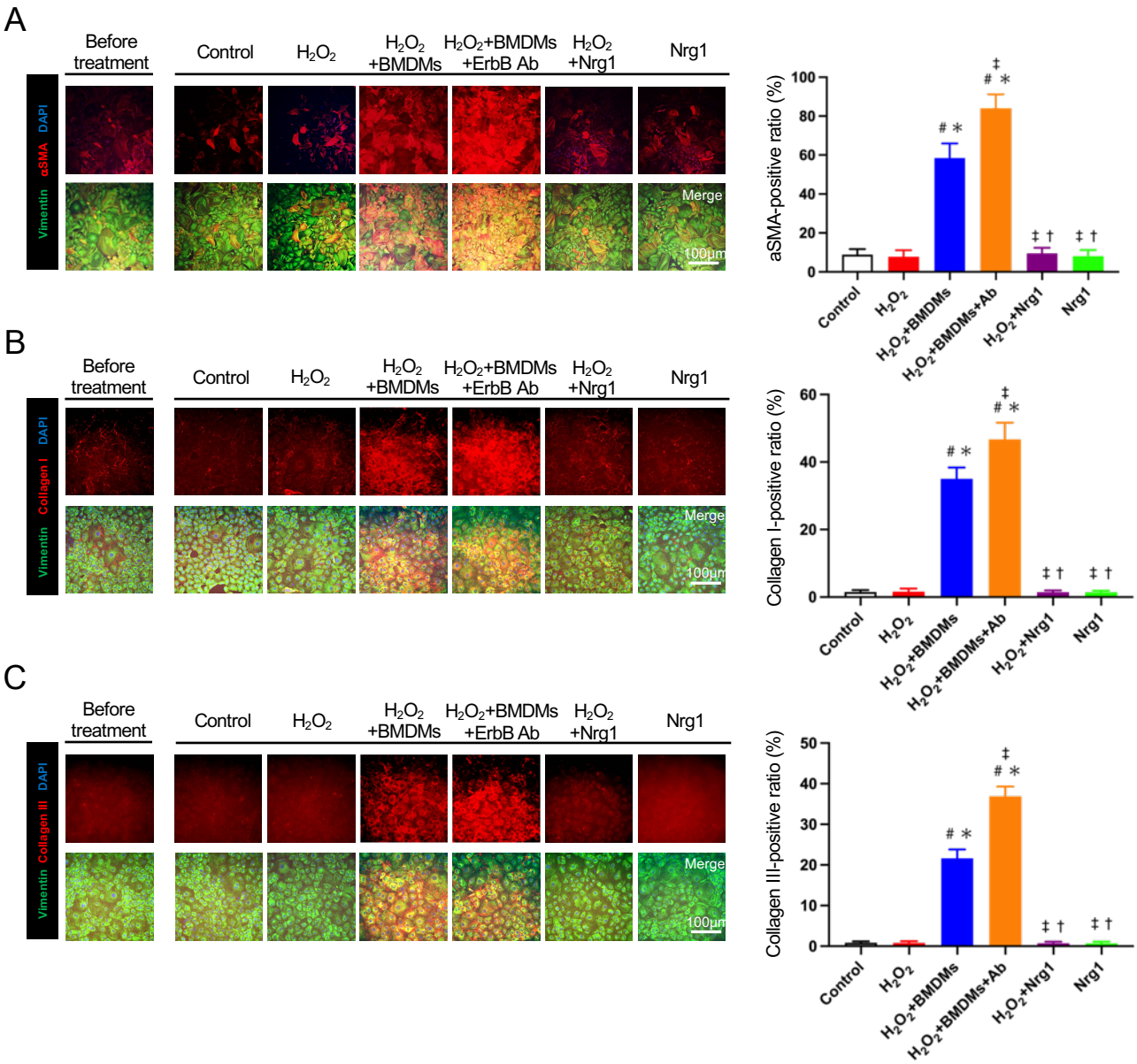
A
Before treatment
Control
H2O2
H2O2 +BMDMs
H2O2+BMDMs +ErbB Ab
H2O2 +Nrg1
Nrg1
DAPI
αSMA
Vimentin
Merge
100μm
aSMA-positive ratio (%)
Control
H2O2
H2O2+BMDMs
H2O2+BMDMs+Ab
H2O2+Nrg1
Nrg1
B
DAPI
Collagen I
Vimentin
Collagen I-positive ratio (%)
C
Collagen III
Collagen III-positive ratio (%)

Figure 5.

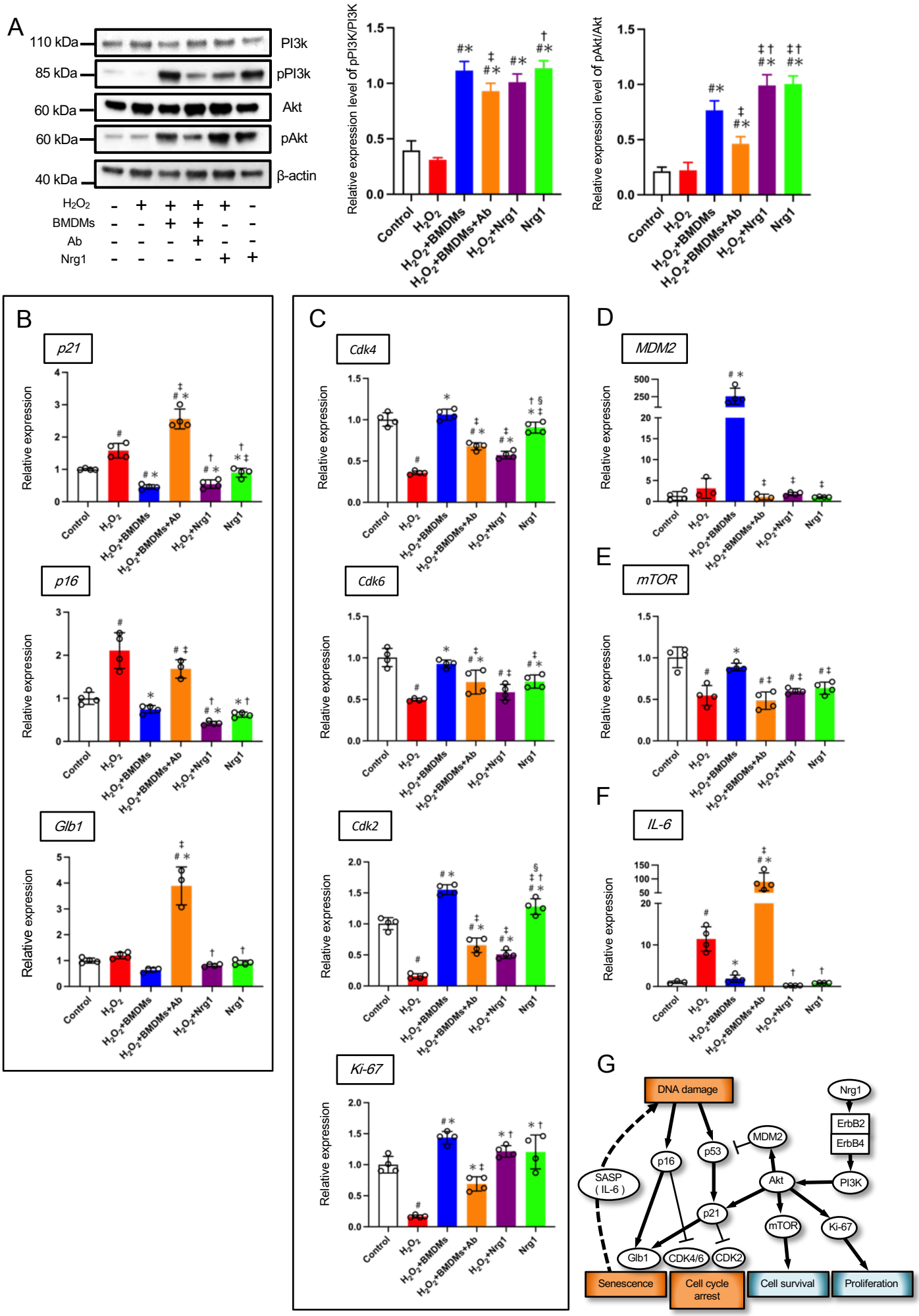
A
110 kDa
85 kDa
60 kDa
60 kDa
40 kDa
PI3k
pPI3k
Akt
pAkt
β-actin
H2O2
BMDMs
Ab
Nrg1
Relative expression level of pPI3K/PI3K
Relative expression level of pAkt/Akt
Control
H2O2
H2O2+BMDMs
H2O2+BMDMs+Ab
H2O2+Nrg1
Nrg1
B
p21
p16
Glb1
C
Cdk4
Cdk6
Cdk2
Ki-67
D
MDM2
E
mTOR
F
IL-6
Relative expression
G
DNA damage
Nrg1
ErbB2
ErbB4
MDM2
p53
p16
SASP
(IL-6)
Akt
PI3K
p21
mTOR
Ki-67
Glb1
CDK4/6
CDK2
Senescence
Cell cycle arrest
Cell survival
Proliferation

Figure 6.

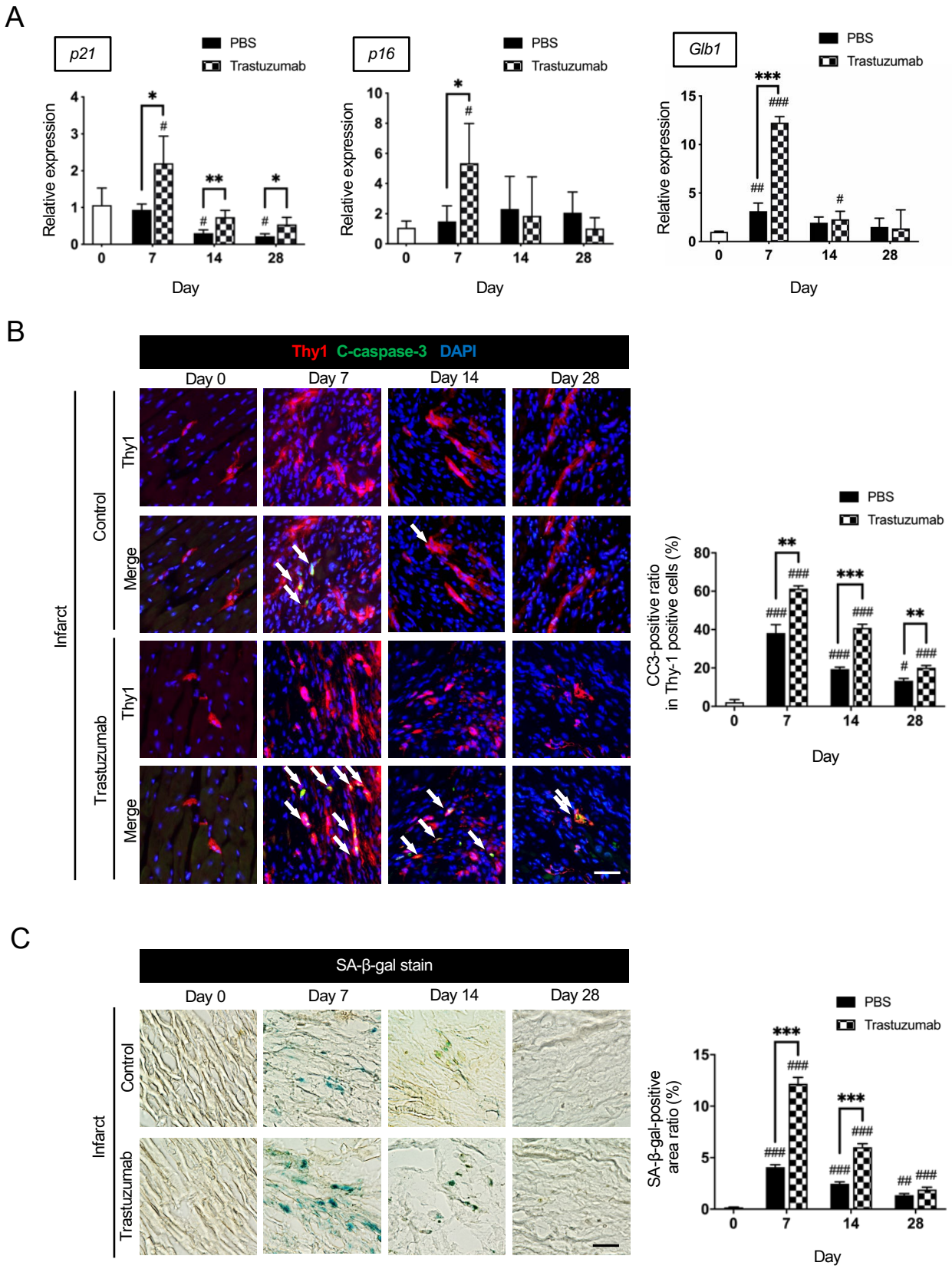
A
p21
p16
Glb1
PBS
Trastuzumab
Relative expression
Day
B
Thy1 C-caspase-3 DAPI
Day 0
Day 7
Day 14
Day 28
Infarct
Control
Trastuzumab
Thy1
Merge
CC3-positive ratio in Thy-1 positive cells (%)
C
SA-β-gal stain
SA-β-gal-positive area ratio (%)

Figure 7.

A

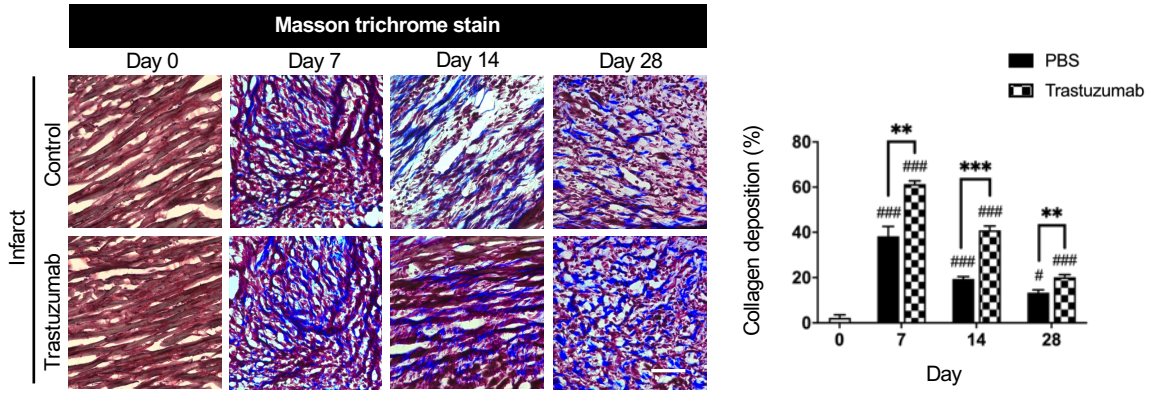
Masson trichrome stain
Day 0
Day 7
Day 14
Day 28
Infarct
Control
Trastuzumab
PBS
Trastuzumab
Collagen deposition (%)
Day

B

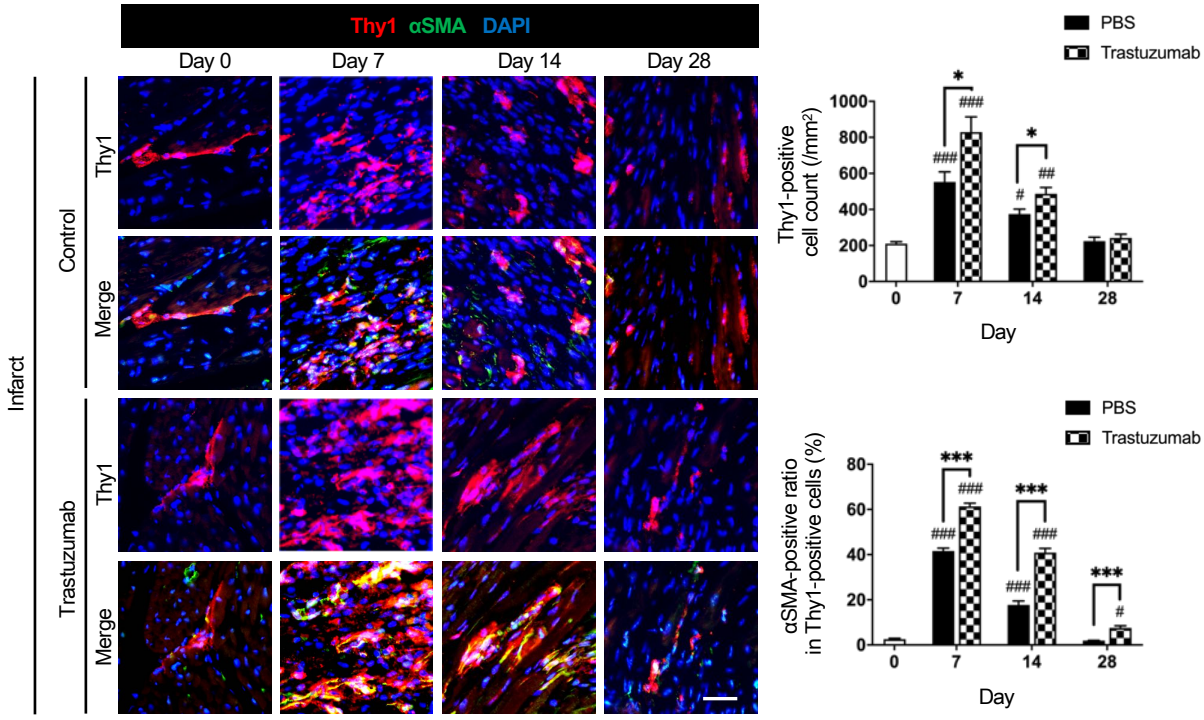
Thy1 αSMA DAPI
Day 0
Day 7
Day 14
Day 28
Infarct
Control
Trastuzumab
Thy1
Merge
PBS
Trastuzumab
Thy1-positive cell count (/mm²)
αSMA-positive ratio in Thy1-positive cells (%)
Day

C

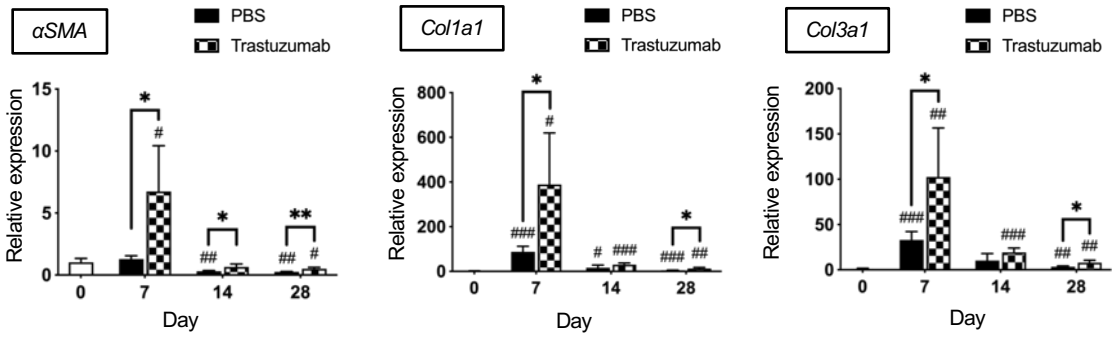
αSMA
Col1a1
Col3a1
PBS
Trastuzumab
Relative expression
Day

Figure 8.

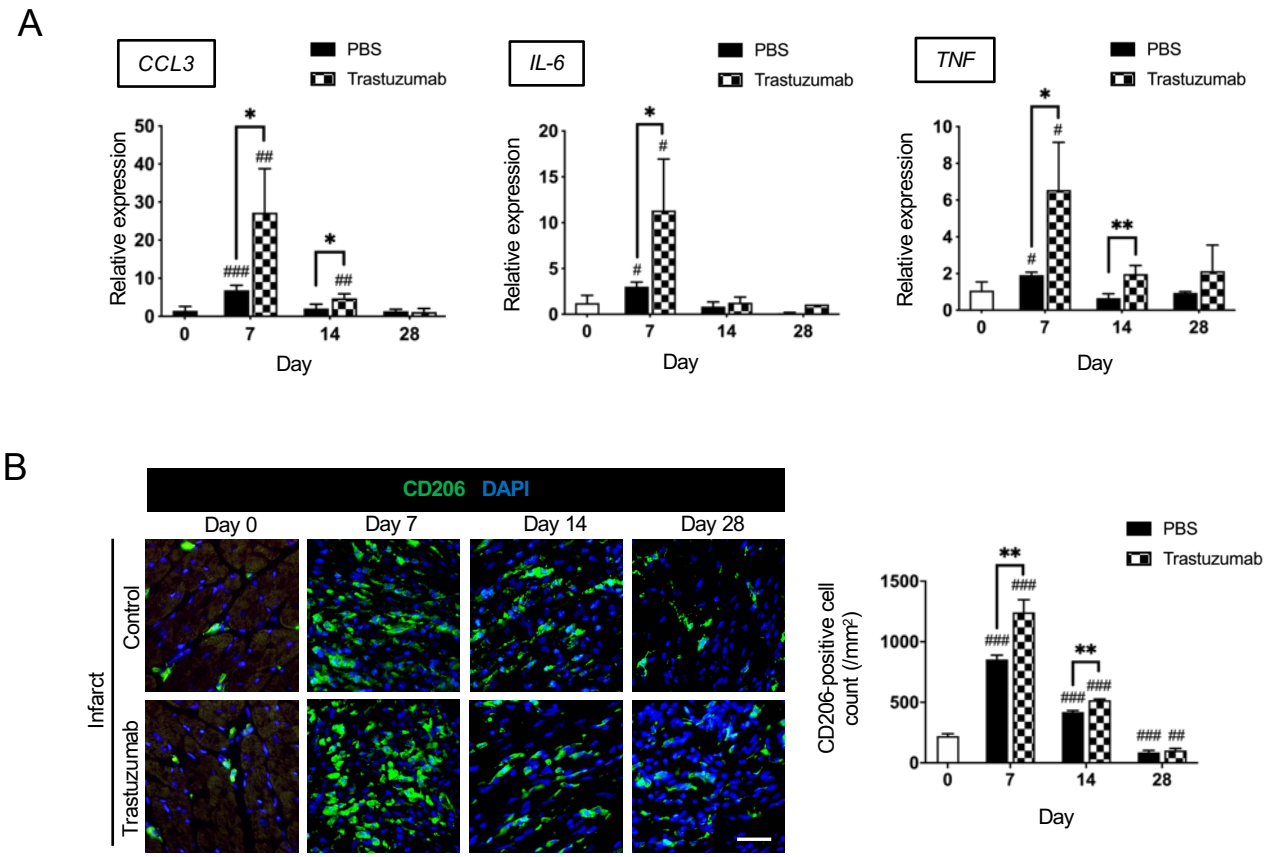
A
CCL3
IL-6
TNF
PBS
Trastuzumab
Relative expression
Day
B
CD206 DAPI
Day 0
Day 7
Day 14
Day 28
Infarct
Control
Trastuzumab
CD206-positive cell count (/mm²)